Mechanical Systems and Signal Processing 106 (2018) 265–283

Contents lists available at ScienceDirect

Mechanical Systems and Signal Processing

journal homepage: www.elsevier.com/locate/ymssp

Vibration energy harvesting based monitoring of an operational bridge undergoing forced vibration and train passage ☆

Paul Cahill [a], Budhaditya Hazra [b], Raid Karoumi [c], Alan Mathewson [d], Vikram Pakrashi [e,f,*]

[a] Centre for Marine and Renewable Energy Ireland (MaREI), Environmental Research Institute, University College Cork, Beaufort Building, Ringaskiddy, Co. Cork, Ireland
[b] Department of Civil Engineering, Indian Institute of Technology Guwahati, Guwahati, Assam 781039, India
[c] Department of Civil & Architectural Engineering, Royal Institute of Technology (KTH), Brinellvägen 23, 10044 Stockholm, Sweden
[d] Heterogeneous Systems Integration, Micro & Nano Systems, Tyndall National Institute, Dyke Parade, Cork, Ireland
[e] Dynamical Systems and Risk Laboratory, School of Mechanical and Materials Engineering and Centre for Marine and Renewable Energy Ireland (MaREI), University College Dublin, Belfield, Dublin 4, Ireland
[f] Marine and Renewable Energy Ireland (MaREI) Centre, University College Dublin, Ireland

ARTICLE INFO

Article history:
Received 31 July 2017
Received in revised form 27 November 2017
Accepted 4 January 2018
Available online 12 January 2018

Keywords:
Energy harvesting
Bridge structure
Full-scale testing
Structural health monitoring
Empirical mode decomposition
Scalogram
Sequential Karhunen Loeve transform
Hilbert transform

ABSTRACT

The application of energy harvesting technology for monitoring civil infrastructure is a bourgeoning topic of interest. The ability of kinetic energy harvesters to scavenge ambient vibration energy can be useful for large civil infrastructure under operational conditions, particularly for bridge structures. The experimental integration of such harvesters with full scale structures and the subsequent use of the harvested energy directly for the purposes of structural health monitoring shows promise. This paper presents the first experimental deployment of piezoelectric vibration energy harvesting devices for monitoring a full-scale bridge undergoing forced dynamic vibrations under operational conditions using energy harvesting signatures against time. The calibration of the harvesters is presented, along with details of the host bridge structure and the dynamic assessment procedures. The measured responses of the harvesters from the tests are presented and the use the harvesters for the purposes of structural health monitoring (SHM) is investigated using empirical mode decomposition analysis, following a bespoke data cleaning approach. Finally, the use of sequential Karhunen Loeve transforms to detect train passages during the dynamic assessment is presented. This study is expected to further develop interest in energy-harvesting based monitoring of large infrastructure for both research and commercial purposes.

1. Introduction

Vibration based structural health monitoring (SHM) of built infrastructure is a topic of significant interest in recent times as the dynamic responses of a structure provide unique insights into its condition and health [1]. With advances in monitoring technology and analysis techniques, there have been many investigations into approaches for the provision of

☆ This paper belongs to the Special issue "Oulu Workshop".

* Corresponding author at: Dynamical Systems and Risk Laboratory, School of Mechanical and Materials Engineering and Centre for Marine and Renewable Energy Ireland (MaREI), University College Dublin, Belfield, Dublin 4, Ireland.
E-mail address: vikram.pakrashi@ucd.ie (V. Pakrashi).

https://doi.org/10.1016/j.ymssp.2018.01.007
0888-3270/

long-term monitoring of civil infrastructure using smart sensing solutions, particularly using wireless sensing solutions [2]. As part of such solutions, the use of vibration based energy harvesting techniques to scavenge electrical energy from the dynamic response of a structure under operational conditions has been shown to have the potential to form the basis of such sensing networks [3,4].

The integration of vibration energy harvesting technology with civil infrastructure is at its infancy [5]. The use of piezoelectric energy harvesting coupled with bridge structures has received attention in this regard, whereby the forced vibration response of a bridge due to vehicular traffic is utilised [6,7]. The amount of energy which can harvested from train-bridge using piezoelectric energy harvesters has also been investigated for an international train fleet [8], as has the application of an energy harvester with train tracks [9]. The use of harvested energy for the purposes of SHM of built infrastructure is promising [10] and the power generated from bridge-vehicle interactions using piezoelectric energy harvesting has been investigated for damage detection in the bridge structure [11]. Such studies have remained mainly theoretical and the potential of using energy harvested from the dynamic responses of built infrastructure for SHM is yet realized. Full-scale implementations and demonstrations of such concepts can address this gap in a robust manner.

Full-scale dynamic assessments of bridges allow for estimating relevant parameters such as mode-shapes, stiffness and damping ratios [12–14]. The use of vehicle induced vibrations as a source of excitation for the bridge structure to determine its dynamic responses has been used extensively, both for highway and train bridges [15–17]. Conducting such assessments is beneficial as the structure is under operational conditions and does not require bridge closure during testing. Issues do arise, however, due to the presence of traffic on the bridge, as the vehicle mass acts as an additional mass on the bridge structure, which can result in variations in the response of the bridge and in the measured natural frequency [18]. The use of ambient vibrations can resolve such issues [19]. Nevertheless, the use of external excitation devices imparting loadings of known magnitude and frequency, while introducing minimal interference to the bridge, is usually the most reliable way to determine relevant parameters of the bridge [20]. Previous shakers utilised for such dynamic testing of bridge infrastructure include vertical excitation using a dropped weight [21], an eccentric mass shaker [22] and a hydraulic shaker [23].

Unlike full-scale dynamic testing of bridges, experimental investigations into the application of energy harvesting technology with full scale bridge structures is a nascent field. The integration of energy harvesting technology with highway bridges have been studied, using both piezoelectric [24] and electromagnetic harvesting devices [25,26]. For train bridge infrastructure, piezoelectric sensors have been implemented for the purposes of weigh-in-motion (WIM) [27]. Aside from this WIM application and determining the power output potential from bridge structures, no full-scale study has investigated how experimentally scavenged electrical energy from bridge structures can be utilised in its own right for monitoring or estimation of system parameters. Such applications can include SHM of a bridge structure using natural frequency, mode shape and curvature/strain mode shape based analysis techniques using dynamical measurements [28]. More recently, the use of wavelet transforms has been utilised successfully for SHM of bridge structures including using numerical models [29], the response of a scaled experimental model bridge subjected to a moving load [30] and the free vibrations following train passages during full-scale dynamical testing [18]. Applications resulting from the use of such techniques on the electrical signal outputs from energy harvesters from civil infrastructure has not yet been achieved.

This paper investigates the deployment of piezoelectric energy harvesting devices for a bridge structure undergoing forced dynamic excitation in its operational conditions and demonstrates how analyses can be carried out on the harvested energy signature to assess important properties related to the bridge. Piezoelectric energy harvesting devices, in the form of cantilever harvesters, were created and calibrated under swept sine loading conditions within a laboratory environment. The harvesting devices were deployed for full scale bridge vibration testing using an external shaker with varying magnitude of swept-sinusoidal excitation. The response of the energy harvesters when coupled with the bridge undergoing controlled forced vibrations is presented and compared against the response of an accelerometer at the harvester locations in this paper. A bespoke data-cleaning for the energy harvesting signature against time, in conjunction empirical mode decomposition (EMD) analysis is observed to be useful for system identification. Additionally, sequential Karhunen Loeve transform is utilised here to determine relevant events on the bridge, like train passage. This paper provides full-scale validation of a piezoelectric energy harvesting devices for monitoring built infrastructure. The paper also attempts to provide guidance around re-creating similar experiments in future for research of commercial applications along with what the expected harvesting signatures and results can be from such tests.

2. Piezoelectric energy harvesting devices for full scale deployment

2.1. Cantilever piezoelectric energy harvesting device

A cantilever piezoelectric harvester device was developed for the purpose of bridge monitoring. The device uses multiple linear cantilevers tuned to different frequencies, thereby resulting in a wide range of frequencies available for effective energy harvesting. This approach addresses issues associated with the narrow bandwidths for optimal energy harvesting for linear piezoelectric energy harvesting devices [31] and allows for effective harvesting over a wider range of frequencies within which the modes of the bridge are estimated to be. Fig. 1 illustrates the general outline of a piezoelectric energy harvesting cantilever, with the device parameters identified, including the length (L), width (w) and the added tip mass (m) along with a photo of such a harvester.

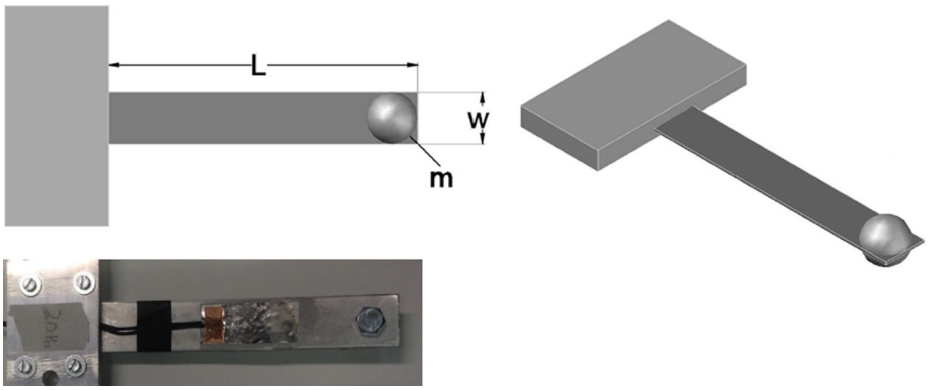

Fig. 1. Schematic design of cantilever piezoelectric energy harvesting device.

The response of the individual cantilever energy harvester can be described through the coupled electromechanical equations [32]:

$$m_h\ddot{z} + c_h\dot{z} + k_h z - \theta V = -m_h\ddot{y}_b \tag{1}$$

$$\theta\dot{z} + C\dot{V} + \frac{1}{R}V = 0 \tag{2}$$

where m_h, c_h and k_h are the effective mass, damping and stiffness of the energy harvester respectively and z is the relative displacement of m_h, with over-dots denoting differentiation with respect to time and $\ddot{y}_b$ is the acceleration from the host structure applied to the rigid base of the device. The electromechanical coupling coefficient for the cantilever is given as θ, V is the voltage output, while C and R are their capacitance and load resistance respectively. The natural frequency of each cantilever, ω, is defined as:

$$\omega = \sqrt{\frac{k_h}{m_h}} \tag{3}$$

while the damping ratio is defined as

$$\xi = \frac{c_h}{2m_h\omega} \tag{4}$$

2.2. Development of energy harvesting cantilevers

To accommodate a wider frequency bandwidth in relation to the host bridge, a total of six piezoelectric energy harvesting cantilevers were constructed, with PolyVinyliDene Fluoride (PVDF) chosen as the piezoelectric material. While PVDF does not possess the same efficiency as other piezoelectric materials, such as PZT, it has a high mechanical strength with excellent flexibility, allowing for robust prototype devices to be created for trial applications. The 52 μm thick PVDF material had a modulus of elasticity, E, of 8.3 GPa, and a piezoelectric constant, e_{31}, of 0.1826 C/m^2. It had silver electrodes, onto which two output solid core wires were attached using copper conductive adhesive tape to record the output voltage. The piezoelectric harvesters were subsequently mechanically bonded onto the surface of the cantilever substrates using an adhesive epoxy. These cantilever substrates were constructed using aluminium, with modulus of elasticity of 69 GPa, and had individually varied geometric properties to achieve different natural frequencies and consequently, different regions of effective energy harvesting. Two such ranges of frequencies were chosen to target the estimated modes of the bridge, with the first frequency range being between 6 Hz and 8 Hz, for Cantilevers 1, 2 and 3, and the second frequency range being between 15 Hz and 20 Hz, for Cantilevers 4, 5 and 6. The physical geometric properties of the individual cantilever energy harvesters are provided in Table 1.

Table 1
Geometric properties of assembled cantilevers (Cant).

Parameter	Cant 1	Cant 2	Cant 3	Cant 4	Cant 5	Cant 6
Length (m)	0.2195	0.2125	0.2545	0.1645	0.1775	0.151
Width (m)	0.0265	0.0265	00.031	0.0257	0.0256	0.0258
Thickness (m)	0.0015	0.0015	0.0015	0.0012	0.0012	0.0012
Mass (kg)	0.0692	0.0683	0.0663	0.0185	0.0191	0.0189

2.3. Natural frequency of individual energy harvesters

An initial experimental calibration was performed to obtain the natural frequency of the individual cantilevers through impulse response experiment. The harvesters were attached to a permanent magnet shaker and the open circuit voltage response was measured for a single impulse load of magnitude 1 g. The voltage response was subsequently determined in the frequency domain using the fast Fourier transform (FFT). For cantilever 1 a peak voltage of 0.158 V was measured, while cantilevers 2 and 3 had peak voltages of 0.153 V and −0.231 V respectively [Fig. 2(a)]. Cantilever 1 had a natural frequency of 7.2 Hz while cantilevers 2 and 3 had natural frequencies of 8.4 Hz and 6.2 Hz, respectively [Fig. 2(c)]. For the cantilevers of the second, higher bandwidth of frequencies, cantilever 4 had peak voltage of 0.81 V, cantilever 5 had a peak of −0.725 V and cantilever 6, a peak voltage output of 0.183 V [Fig. 2(b)]. The corresponding natural frequencies were determined to be 17.6 Hz, 15.8 Hz and 20.6 Hz respectively [Fig. 2(d)]. The lower magnitude of cantilever 3 in the frequency domain is explained by the fact that maximum energy was concentrated around a peak close to 25 Hz [Fig. 4]. The experimental frequencies were determined to be satisfactory for the application of the device to the host bridge structure, as the exact frequency of the structure was only approximately estimated before the commencement of the dynamic testing. Following this initial calibration to determine the natural frequency, a more detailed experimental calibration was performed to determine the voltage response of the devices for varying loading conditions.

2.4. Calibration of energy harvesting devices

The test plan for the deployment of the energy harvesting devices involved forced vibration of the host bridge over a wide loading frequency range. Consequently, the response of the energy harvesting devices to loadings of different frequencies was investigated. To calibrate the devices, a swept sine frequency loading was applied to the base of the energy harvesters using a permanent magnet shaker. Sinusoidal loads were applied at increasing frequencies ranging from 1 Hz to 40 Hz at a constant amplitude over a total time of 120 s.

The response of individual cantilevers for the lower range of frequencies were measured for the loading described [Fig. 3]. The response of each cantilever shows a maximum voltage at a frequency of loading equal to the natural frequency of individual cantilevers. All three of these natural frequencies match with their corresponding impulse load calibration. The maximum voltage output for cantilevers 1 and 2 were 0.139 V and 0.182 V respectively, with the peak voltage outputs occurring about the natural frequency, at 7.4 Hz for cantilevers 1 and 8.5 Hz for cantilever 2. The voltage at the natural frequency for cantilever 3 was 0.0631 V occurring at a frequency of 6.2 Hz, however the maximum voltage obtained was 0.066 V at a loading frequency of 39.5 Hz.

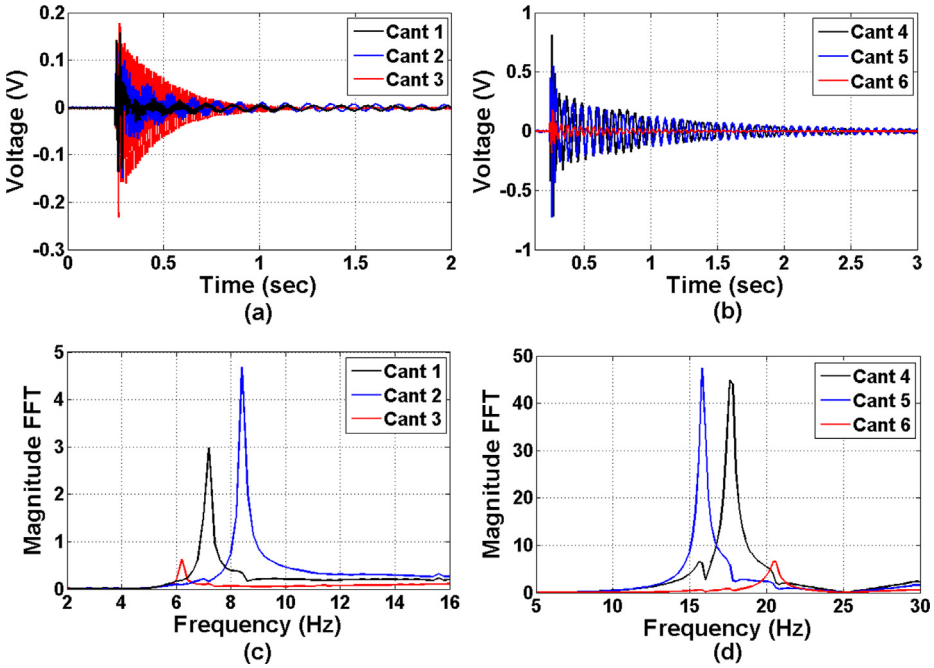

Fig. 2. Voltage response of devices due to impulse load for (a) Cantilevers 1, 2 and 3, (b) Cantilevers 4, 5 and 6; and resultant FFT for (c) Cantilevers 1, 2 and 3, (d) Cantilevers 4, 5 and 6.

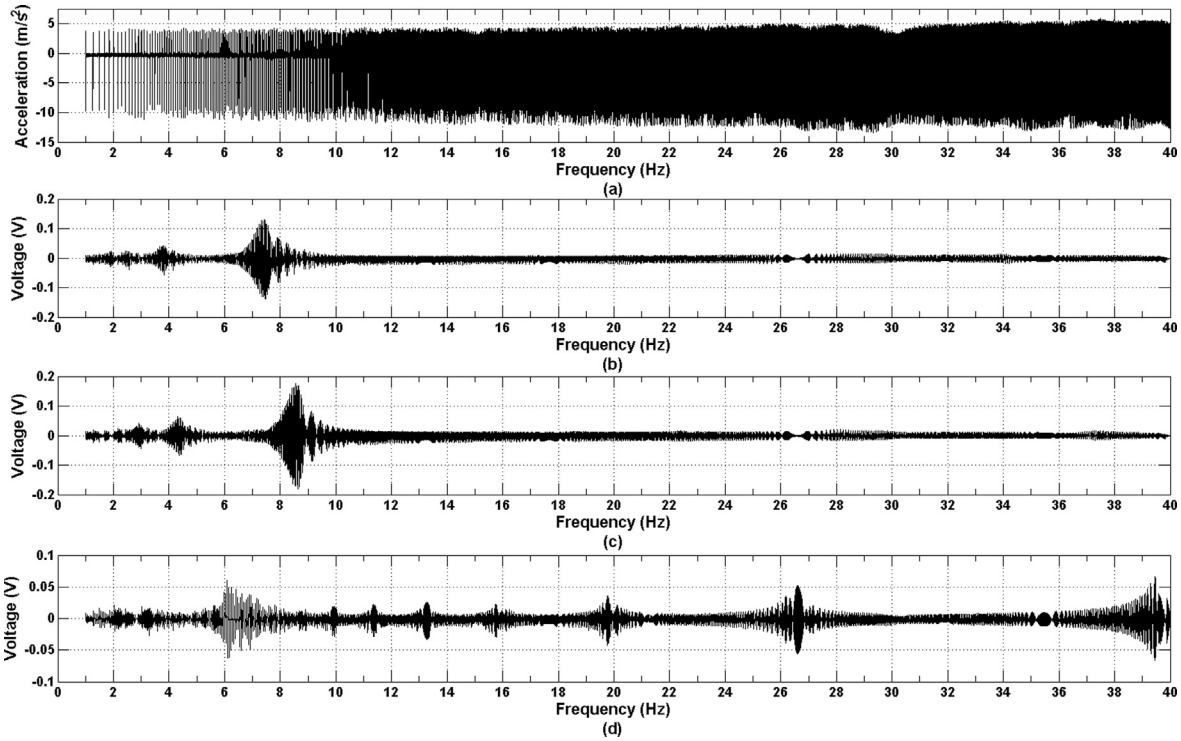

Fig. 3. Response of harvesters subjected to swept frequency loading with (a) Base excitation and voltage output of (b) Cantilever 1, (c) Cantilever 2 and (d) Cantilever 3.

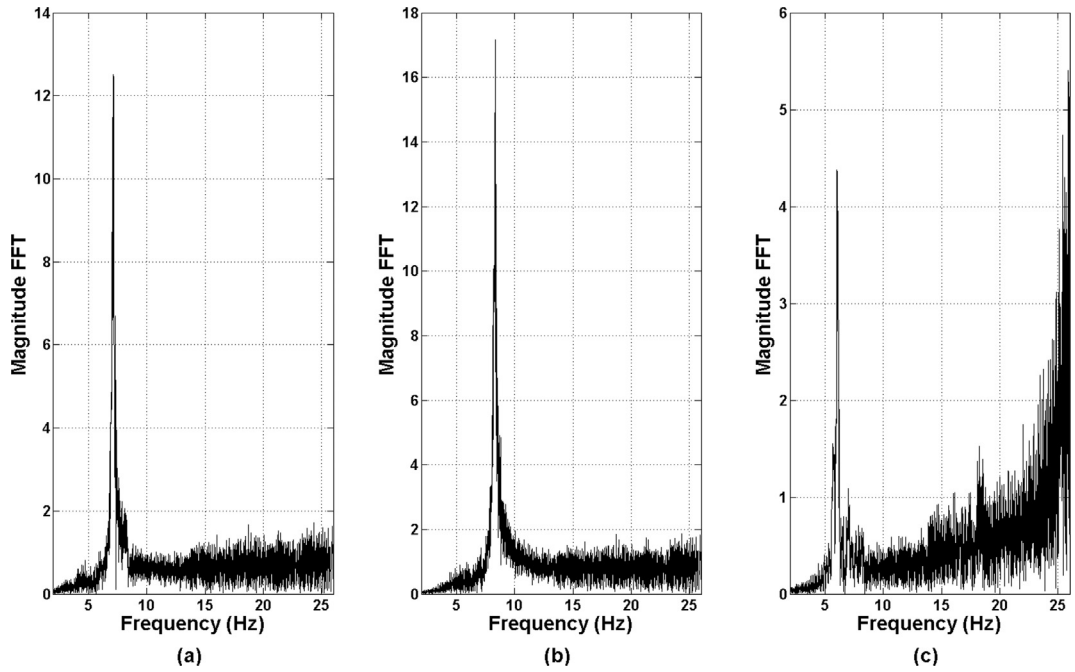

Fig. 4. FFT analysis of harvesters subject to swept frequency loadings for (a) Cantilever 1, (b) Cantilever 2 and (c) Cantilever 3.

FFT analysis yielded the frequency domain response of the harvesters from the swept sinusoidal applied loading [Fig. 4]. Cantilevers 1 and 2 result in a maximum response magnitude corresponding to their natural frequencies, with magnitudes of 12.51 and 17.17 occurring at 7.11 Hz and 8.37 Hz respectively. Cantilever 3, however, shows a maximum peak at the cut off frequency of 26 Hz, with a second peak at the 6.09 Hz corresponding to a magnitude of 4.37.

The harvesters of the second frequency range were investigated next, with calibration performed with applied loadings conditions similar to what has been previously described. The maximum voltage of cantilever 4 was found to be 1.626 V and for cantilevers 5 and 6, the maximum voltages were 1.594 V and 0.348 V respectively [Fig. 5]. The maximum voltage for each cantilever was obtained close to the natural frequencies, as expected.

The analysis of the voltage output of the harvesters of the second frequency bandwidth using FFT also shows their responses to be in keeping with the previous results, with all peaks being at the respective natural frequencies [Fig. 6]. For cantilever 4, at a frequency of 17.95 Hz, the maximum amplitude was 98.06, for cantilever 5, at a frequency of 15.75 Hz, a maximum amplitude of 118.85 was measured and, finally, for cantilever 6, a maximum amplitude of 23.56 was found at a frequency of 20.45 Hz. The drop of voltage of cantilever 6 is not obvious in terms of explanation but is likely to be related to the quality of adhesion of the PVDF material to the cantilever itself, thereby reacting to the dynamic responses of the host structure but with a significantly reduced value of harvested energy in terms of voltage, which in turn is reflective of the dynamic strain occurring in the PVDF material.

3. Host bridge structure for energy harvesting applications

3.1. Details of host bridge structure

The Pershagen Bridge, Sweden was chosen for the deployment of energy harvesters. This bridge is a 46.6 m long slab double track rail bridge, consisting of three spans and four supports [Fig. 7(a)]. The main central span is 18.4 m in length and the two side spans have a length of 11.1 m. An overhang exists between the side-spans and the abutments, which rest on backfill embankments. The bridge is 11.9 m in width out to out and carries ballast of depth 0.6 m atop of the reinforced concrete slab deck, above which rests the train tracks [Fig. 7(b)]. Due to the overhangs at either end of the bridge, and their respective foundations within the embankments, the bridge exhibits some cantilever-like behaviour when subjected to dynamic loads. The results of such behaviours renders the dynamic modelling of the bridge structure difficult to achieve accurately without performing model updating using forced dynamic testing to determine structural parameters [33].

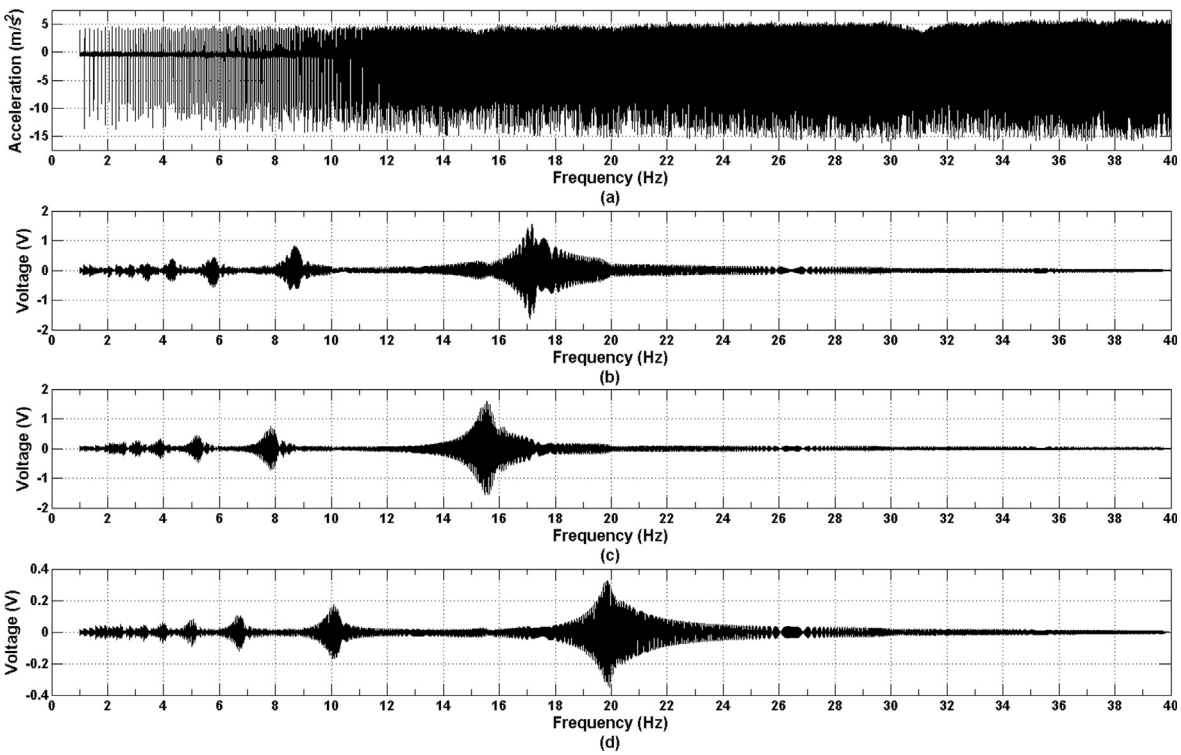

Fig. 5. Response of harvesters subjected to swept frequency loading with (a) base excitation and voltage output of (b) Cantilever 4, (c) Cantilever 5 and (d) Cantilever 6.

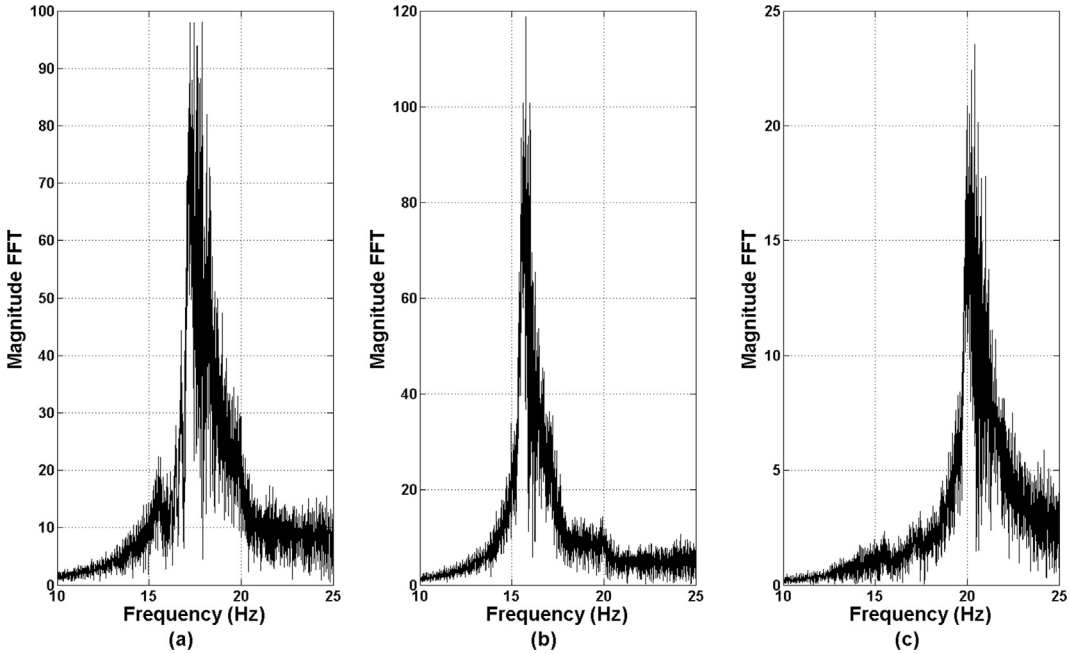

Fig. 6. FFT analysis of harvesters subject to swept frequency loadings for (a) Cantilever 4, (b) Cantilever 5 and (c) Cantilever 6.

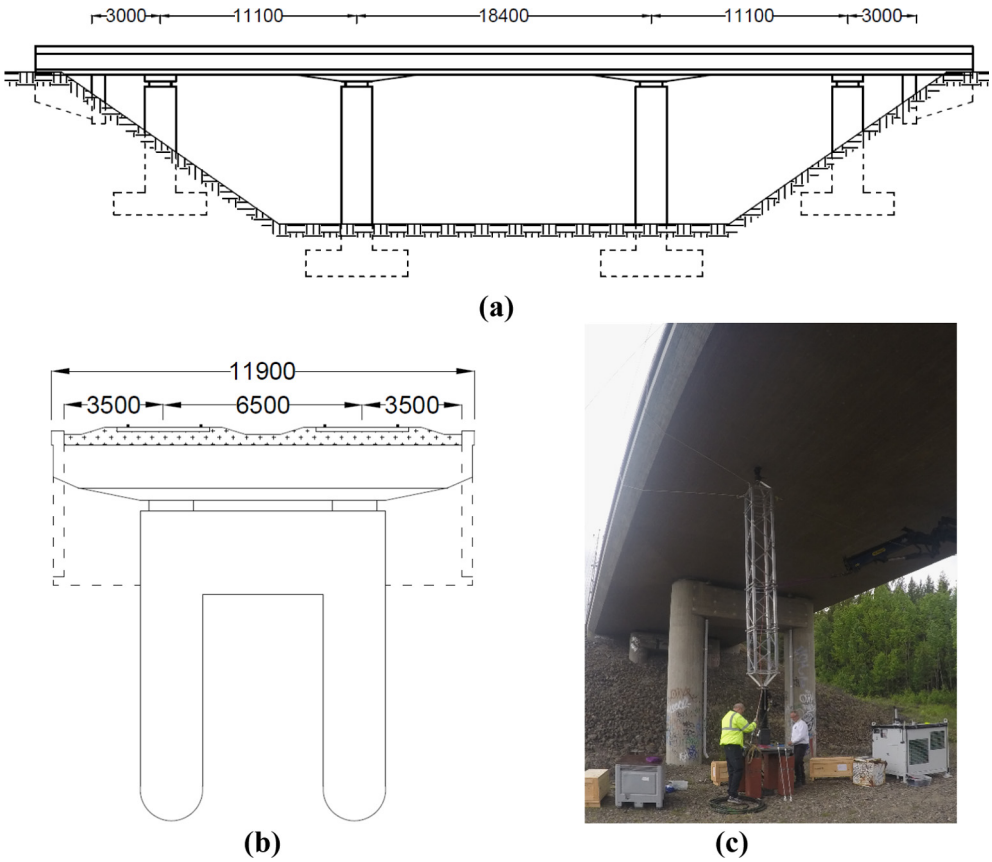

Fig. 7. Schema of host bridge structure with (a) Side elevation, (b) Front elevation and (c) Hydraulic shaker unit.

The shaker unit used to excite the Pershagen Bridge is a hydraulic shaker designed by the Division of Structural Engineering and Bridges at KTH Royal Institute of Technology, Sweden. It consists of a hydraulic cylinder with an attached strut [Fig. 7 (c)], atop of which is a load cell providing a feedback loop. This allows for the desired force, frequency and displacement of the load being applied to the bridge structure to be constantly maintained. Consequently, the shaker can apply a swept sinusoidal loading of varying magnitudes to the connected bridge, with further information on the shaker available from [34]. Of note is the positioning of the shaker below the bridge superstructure, which allows for the bridge to remain open to traffic during the forced dynamic testing of the bridge. This marks an important development in dynamical testing of bridges as any issue with regards disruption to services is no longer then a factor of concern.

3.2. Deployment of energy harvesting devices during forced dynamic testing

The location of the energy harvesting devices was chosen based on the proximity of the positions of the shaker unit and to an accelerometer. This criterion was based on two key factors. The first factor was in consideration of the magnitude of the base excitation from the dynamic shaker, which the devices are subject to. The second factor was in relation to providing reference acceleration measurements of the base excitations experienced by the devices obtained from an accelerometer.

The shaker unit was placed 2.4 m from the longitudinal midspan of the main central span and 3.45 m from the edge of the bridge [Fig. 8(a)]. A preload was applied by the shaker between the ground and the bridge, to ensure constant contact between the two during dynamic testing. To determine the response of the bridge to such tests, an array of nine uniaxial accelerometers were mounted along its top edge beams, with data collected using a HBM MGCPlus data acquisition system at a sampling frequency of 600 Hz. Based on the previous described criterion for placement, the two devices were mounted to the bridge at a Position A, as identified in Fig. 8 as Pos. A. This included an accelerometer, which was in closest proximity to the shaker unit. The devices were affixed to the top edge beam of the bridge [Fig. 8(b)], with the accelerometer centred at the midpoint between the devices. The devices were placed so that the cantilevers were overhanging the bridge, to prevent them coming into contact with the deck or other items [Fig. 8(c)]. The response of the devices was monitored and recorded at a sampling rate of 100 Hz.

3.3. Dynamic testing procedure for host bridge structure

A total of three sets of tests were completed on the bridge. The first and second tests were carried out at two different loading magnitudes with a similar frequency range and rate of loading applied for both. Such a test is important for the detection of any non-linearity in the dynamic response of the bridge. The third and final test was conducted at a reduced loading rate over a narrow frequency range, centred about the estimated natural frequency to obtain a more thorough description of the first mode shape. The test details are summarised in Table 2.

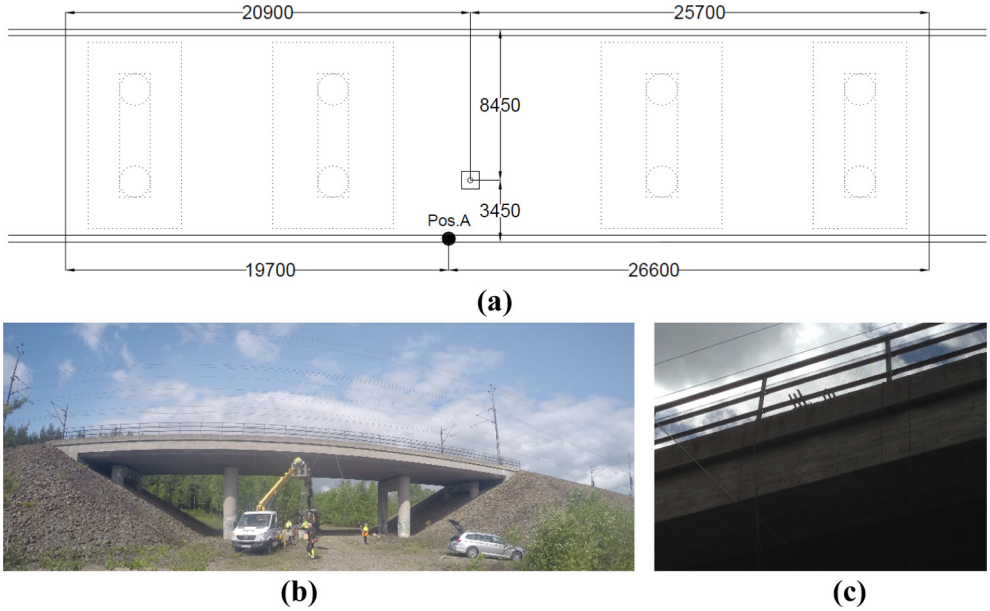

Fig. 8. Deployed energy harvesting devices including (a) Location of energy harvesting devices (Pos. A) and shaker unit, (b) Image of bridge structure and (c) image of deployed energy harvesting devices.

Table 2
Details of applied loadings during dynamical testing of host bridge.

Test	Applied pre-load (kN)	Load amplitude (kN)	Frequency range (Hz)	Loading rate (Hz/s)
Test 1	15	5	3–50	0.05
Test 2	15	10	3–50	0.05
Test 3	15	10	5–10	0.01

4. Experimental results from dynamic testing of bridge structure

4.1. Acceleration response of bridge during dynamic testing

The acceleration response of the bridge at Position A was measured for three dynamic tests. A comparison of Test 1 and Test 2, which had the same frequency range and loading rate but different magnitudes, indicates that a significantly high response was recorded at 78 s during both tests, with a peak magnitude of 0.34 m/s^2 and 0.63 m/s^2, respectively [Fig. 9 (a) and (b)]. Otherwise, both tests have incidental peaks as responses due to train passages occurring during the forced dynamic testing, at times centred about 54, 295 and 590 s for Test 1, and 580, 723 and 775 s for Test 2 respectively. These incidents resulted in a maximum acceleration response of −1.94 m/s^2 and −1.59 m/s^2 for Test 1 and 2 respectively. Test 3, with a smaller frequency range and lower loading rate compared to the two previous tests, had a high response recorded between 250 and 300 s. The peak magnitude was 0.71 m/s^2. A single incident peak due to a train passage occurred at 225 s and resulted in a maximum acceleration response of 1.81 m/s^2 [Fig. 9(c)].

The frequency domain response of the measured acceleration during the three tests was obtained using FFTs, with all three tests resulting in a maximum amplitude occurring in the region of 7.8 Hz. Test 1 resulted in a maximum amplitude of 494.7 at 7.873 Hz, Test 2 registered a maximum amplitude of 817.3 at 7.805 Hz and Test 3 had a maximum amplitude of 1887.6 at 7.794 Hz [Fig. 10]. From all three tests, the natural frequency of the bridge is identified to be in the region of 7.8 Hz, with further modes identifiable at higher frequencies.

4.2. Voltage response of energy harvesting devices during dynamic testing of bridge structure

For Test 1, it was found that the cantilevers of the first, lower bandwidth, recorded an event profile similar to that obtained by the accelerometer but with signal outputs that contained more noise [Fig. 11]. All three cantilevers recorded

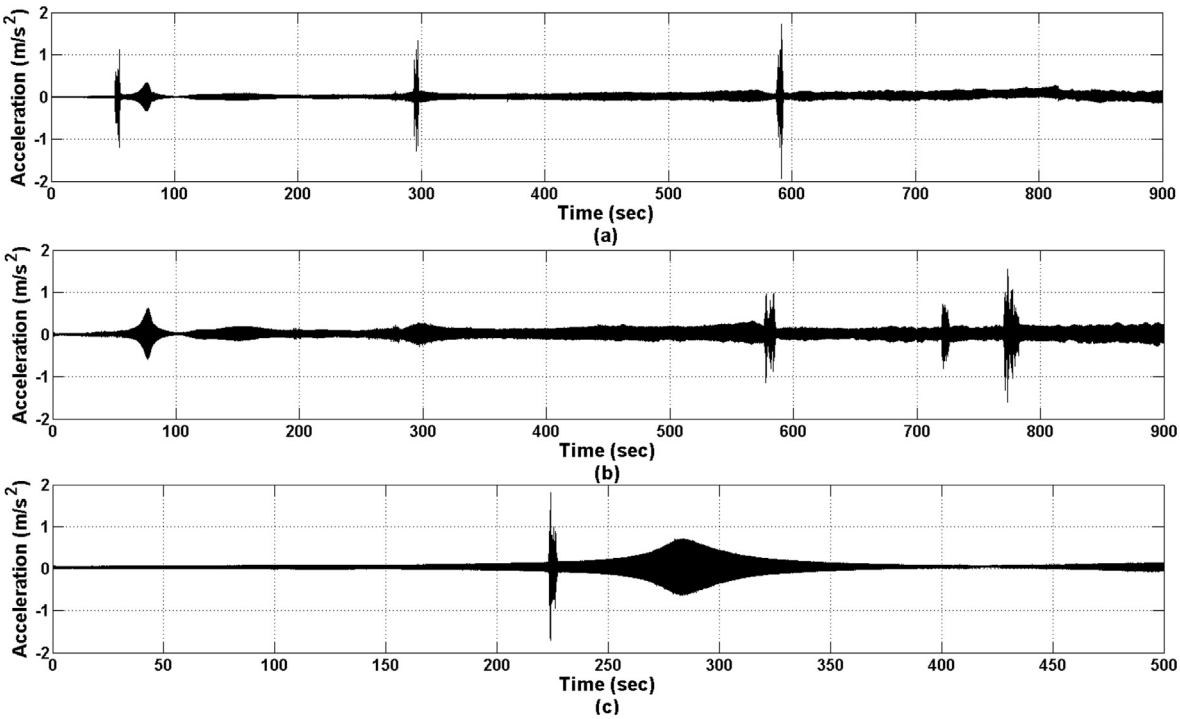

Fig. 9. Time based recordings from accelerometer at Position A for (a) Test 1, (b) Test 2 and (c) Test 3.

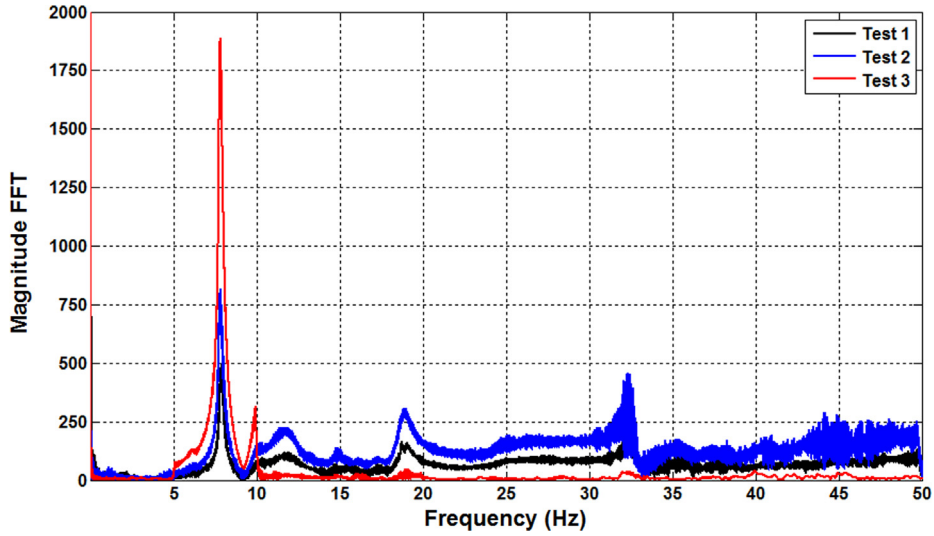

Fig. 10. FFT analysis of accelerometer output at Position A resulting from Tests 1, 2 and 3.

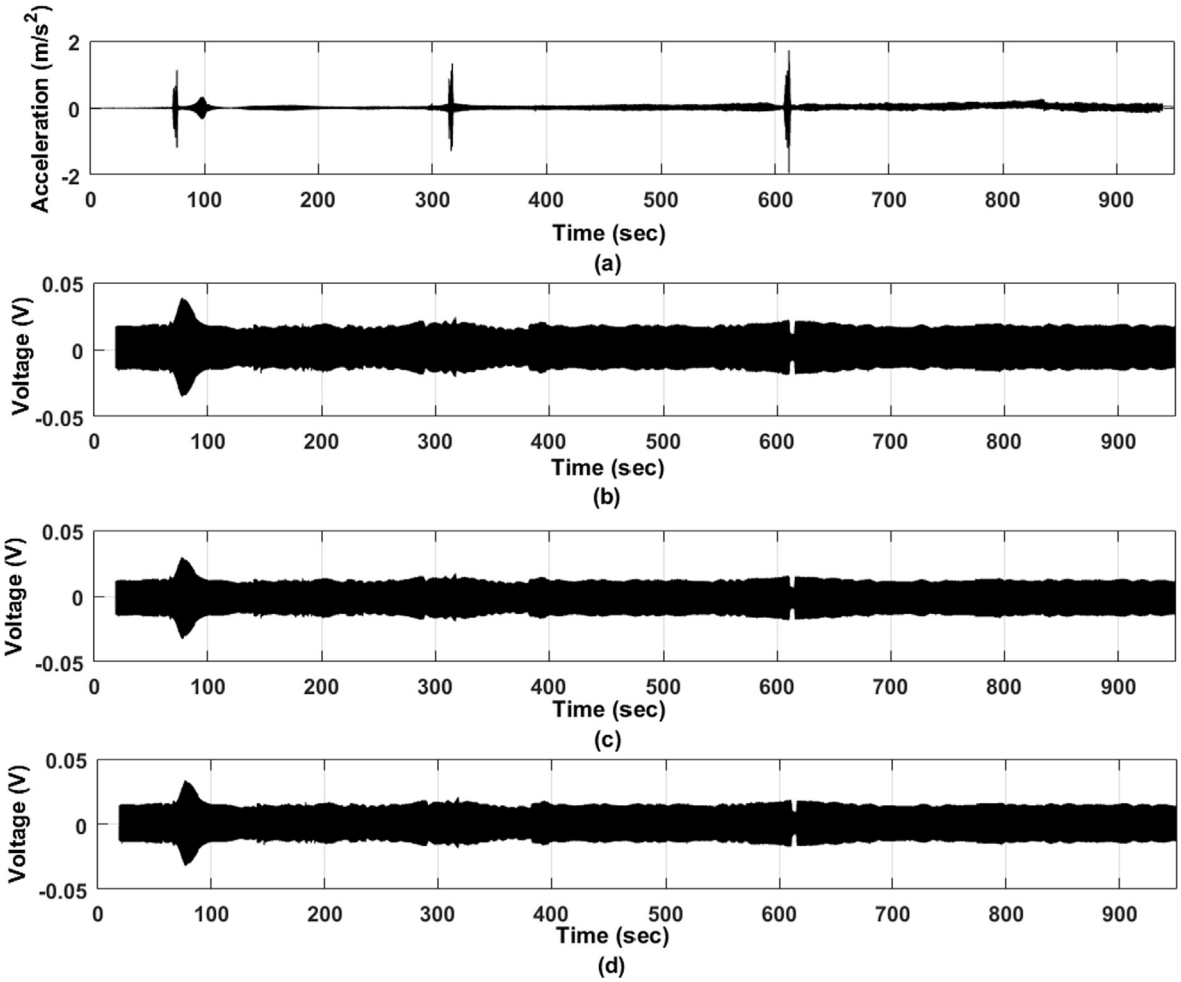

Fig. 11. Results for Test 1 including (a) Acceleration and voltage response from (b) Cantilever 1, (c) Cantilever 2 and (d) Cantilever 3.

a similar voltage output profile. A maximum voltage output occurred at about the 80 s mark of the test, corresponding to 0.039 V, 0.032 V and 0.032 V for cantilevers 1, 2 and 3 respectively. The three train events which were recorded during the test by the accelerometer were also found to have been picked up by the energy harvesting devices.

The voltage output response resulting from Test 1 was obtained similarly for the three energy harvesting cantilevers of the second frequency bandwidth [Fig. 12]. As was the case for the previous harvesters, there is good correlation between the accelerometer based events and the responses obtained from individual cantilevers. These events are more distinct in the response of the three harvesters with the higher bandwidth when compared to those of the lower bandwidth, due to the magnitude of the voltage output being higher during such events. The maximum voltage responses obtained were 0.053 V, 0.071 V and 0.052 V for cantilevers 4, 5 and 6 respectively.

The response of the harvesters within the first bandwidth of frequencies during Test 2 was not in keeping with the previous response from Test 1, with a low response for the first half of the dynamic loading recorded for all three cantilevers [Fig. 13]. The response in detecting the events for the latter half of the test was, however, better, with three events registering a response compared to the acceleration profile at 580, 720 and 775 s. The maximum voltage output for cantilevers 1, 2 and 3 were 0.064 V, 0.053 V and 0.055 V respectively.

A similar trend was observed for the three harvesters with higher frequencies during Test 2, with events occurring in the first half of the test not being as prominent as observed during Test 1. The maximum voltage outputs during Test 2 were 0.099 V, 0.144 V, 0.091 V for cantilevers 4, 5 and 6 respectively [Fig. 14]. As with the previous harvesters, events at 580, 720 and 775 s detected by the accelerometer are also detected by all three cantilevers of device 2. Similar to Test 1, the harvesters with higher frequencies provide a better response when compared to those with lower frequencies.

Test 3 was conducted over a shorter frequency range of excitation load and with a lower rate of loadings as compared to Tests 1 and 2. The voltage outputs from the first three harvesters during Test 3 show a low response from the cantilevers when compared to the accompanying acceleration measurements [Fig. 15]. None of the cantilevers appear to have detected either the forced vibrations from the shaker unit or the train event recorded at 235 s. An event is detected between 170 and 220 s by all three cantilevers, but this is not detected by the accelerometer. The maximum voltage output from cantilevers 1, 2 and 3 during Test 3 are 0.029 V, 0.024 V and 0.025 V respectively.

Similar results were obtained for the three harvesters with higher frequencies during Test 3. The correlations between the recorded acceleration and the voltage response from cantilevers 4, 5 and 6 [Fig. 16] are small. Maximum voltage responses of 0.030 V, 0.050 V and 0.029 V were obtained from cantilevers 4, 5 and 6. While events recorded by the accelerometer were not reflected in the response of the cantilever, the event detected between 170 and 220 s by the three harvesters of lower frequencies is also detected by the cantilevers within the higher frequency range.

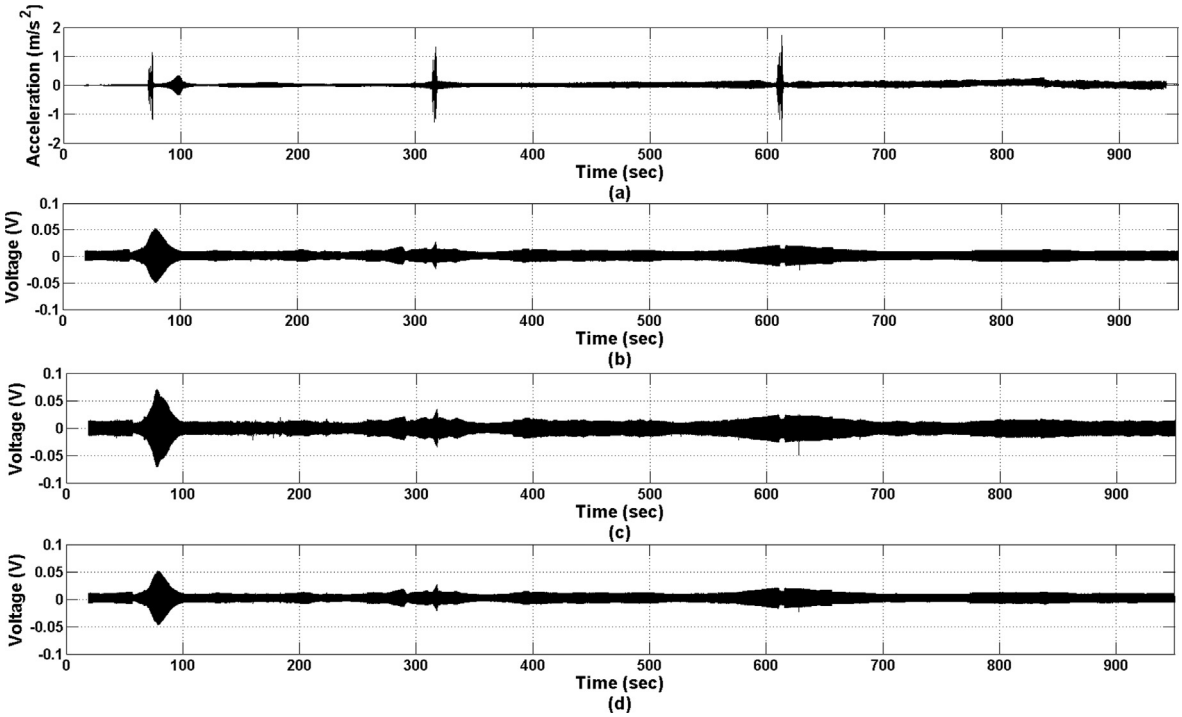

Fig. 12. Results for Test 1 including (a) Acceleration and voltage response from (b) Cantilever 4, (c) Cantilever 5 and (d) Cantilever 6.

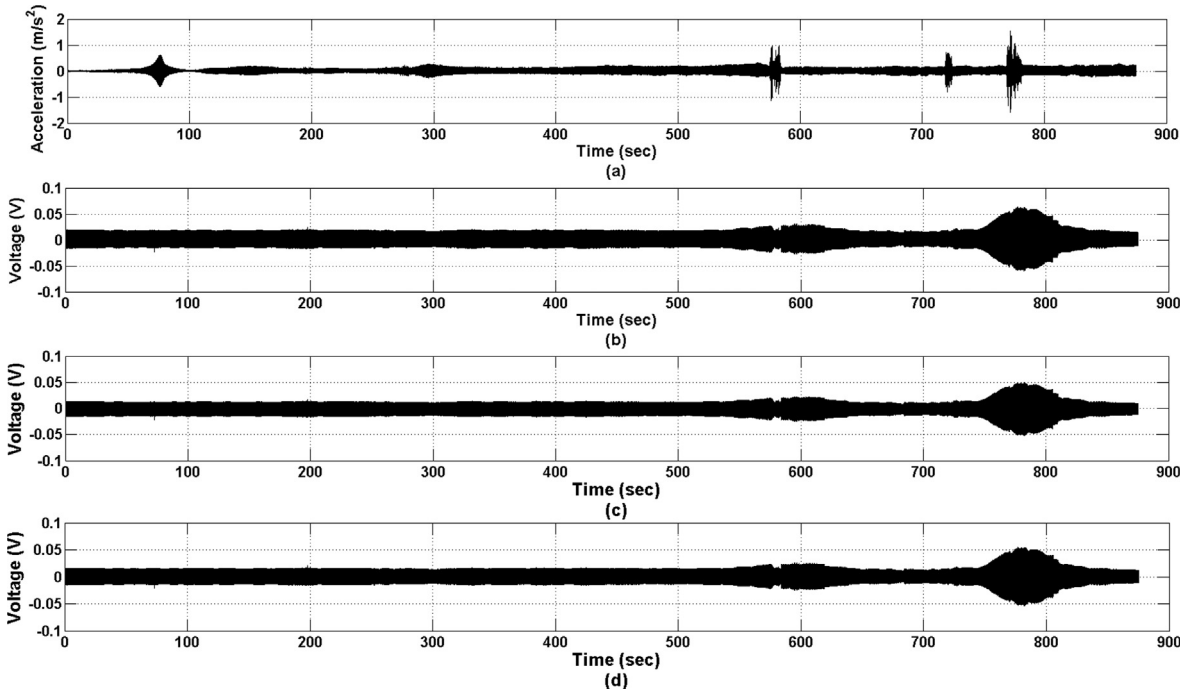

Fig. 13. Results for Test 2 including (a) Acceleration and voltage response from (b) Cantilever, 1 (c) Cantilever 2 and (d) Cantilever 3.

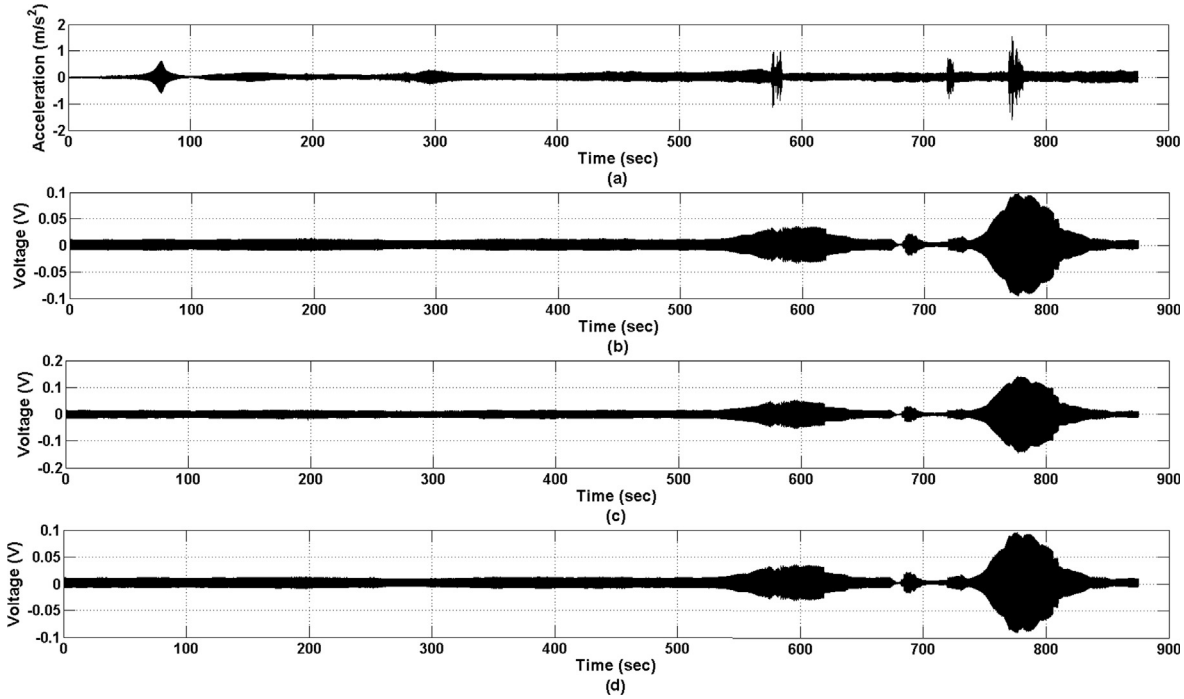

Fig. 14. Results for Test 2 including (a) Acceleration and voltage response from (b) Cantilever 4, (c) Cantilever 5 and (d) Cantilever 6.

5. Analysis of voltage output data

In this section the analysis of the harvester data is discussed considering its characteristic features, along with processing undertaken to make it amenable for the identification of the modes of the bridge, as well as other important features like

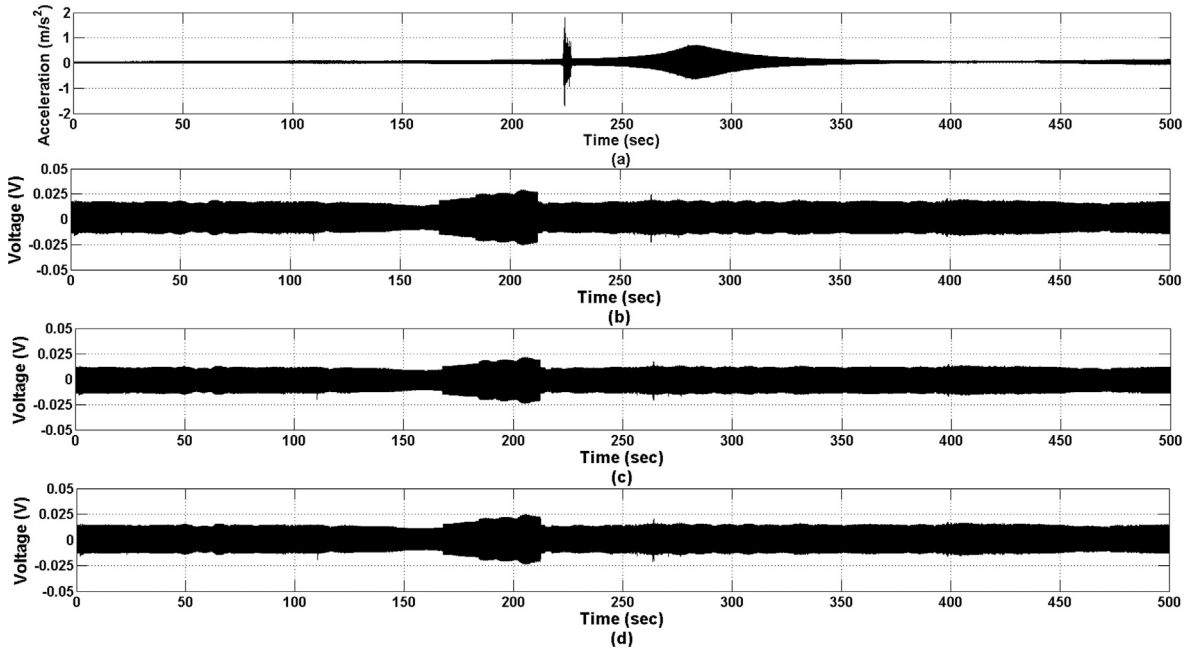

Fig. 15. Results for Test 3 including (a) Acceleration and voltage response from (b) Cantilever 1, (c) Cantilever 2 and (d) Cantilever 3.

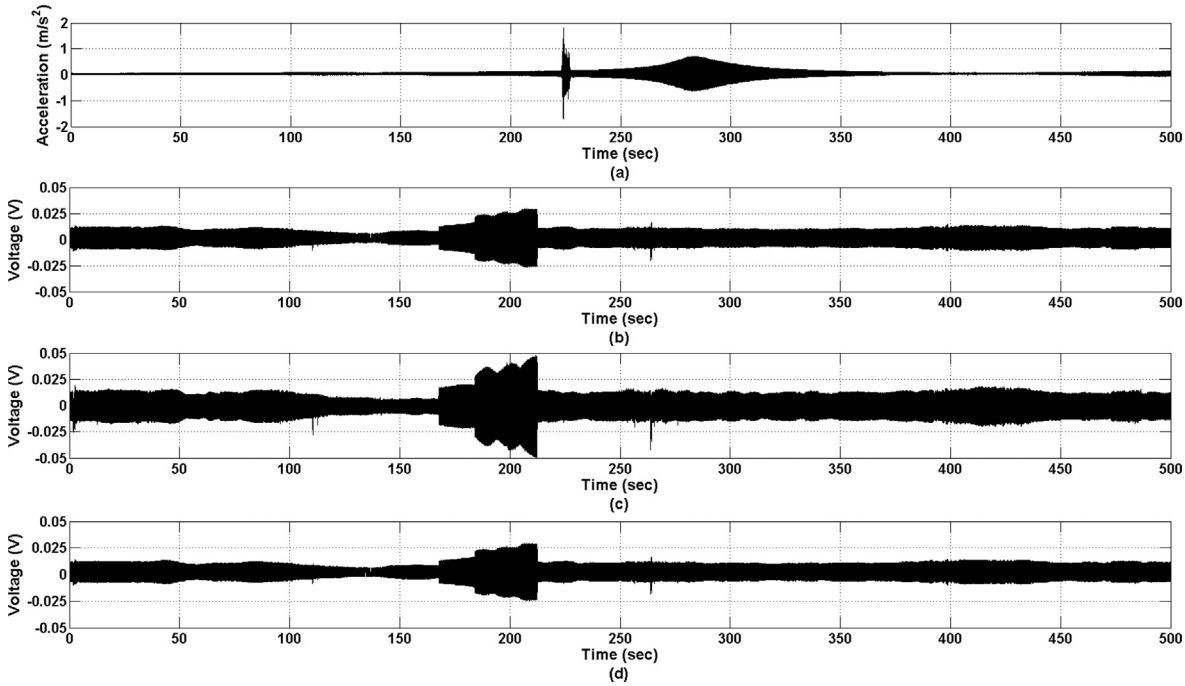

Fig. 16. Results for Test 3 including (a) Acceleration and voltage response from (b) Cantilever 4, (c) Cantilever 5 and (d) Cantilever 6.

train passage. As previously outlined, dynamic tests were carried out using swept sinusoidal excitations at designated sweep rates between the starting and ending frequency. However, caution needs to be exercised while interpreting the data, which includes ambient environmental effects. The tests were carried under significantly steady mean wind fields with strong wind gusts. Therefore, it is not unnatural to expect presence of noise in the data as well as the behaviour of the modes from being localized in both time and frequency domain, to being localized in frequency domain only, thereby indicative of a strong influence of ambient broadband excitation. Once the raw data is analysed, suitable schemes to denoise the data are discussed

followed by an Empirical Mode Decomposition (EMD) based identification [35]. As a closure, an algorithm based on the use of feature indicators and sequential Karhunen Loeve transform [36] to detect real time train passage is discussed.

5.1. Analysis of the raw data and denoising

Fig. 17 shows the windowed spectra, scalogram and the time series data of cantilever 4 subjected to a sweep rate of 0.05 Hz/s for the windows 1 and 10. It is observed that there is a significant energy concentration corresponding to the peak at 16.6 Hz. However, it is also apparent from the subplots (b) and (c) that the 16.6 Hz is a pure non-decaying sinusoid, thereby precluding the possibility of any mode. This sinusoid is mostly the line noise or the noise frequently encountered while dealing with AC current/voltage sources associated with the power source used to run the shaker. At the same time, it is also evident from Fig. 17, that the energy of the 16.6 Hz peak is significant to the extent that it masks all the other vibrating frequencies. Hence it is imperative that the data is band-passed between 0–16 Hz and 17–35 Hz to examine the vibrating components in the frequency and the time-frequency domain.

Fig. 18 shows the band-pass filtered cantilever 4 harvester data corresponding to the two pass bands (a) 0–16 Hz and (b) 17–35 Hz. The presence of sharp spikes can be clearly observed throughout the data and can severely affect the efficacy of the modal identification.

A spike removal algorithm is therefore proposed that makes use of Hilbert transform to extract the modulation of the data, demodulate the data by dividing the raw data by the extracted envelop, use mean plus 3 times standard deviation thresh-holding on the envelop, smoothening and finally multiplying the smoothened envelop to the demodulated data. The steps of denoising are as follows:

- Envelop is extracted from the input data by using Hilbert transform
- The input data is demodulated by dividing the data with the envelop
- Thresholding is applied to reduce the effect of spikes. Mean plus 3 times standard deviation is applied
- The thresholded envelop is further smoothened using Savitzky-Golay filter of order 3 using 27 windows
- The smoothened envelop is now multiplied element-wise with the demodulated data.

The results of such denoising is in Fig. 19, illustrating the bandpassed time series as described in Fig. 18, compared with the output signal following the denoising procedure outlined above.

5.2. Modal identification

Modal identification was carried out by using EMD applied on single channel harvester data. EMD has been extensively applied for modal identification of vibrating systems subjected to ambient excitation [37,38]. It is well understood that EMD when applied without bandpass filtering or intermittency criterion, causes significant mode-mixing. In the present work, EMD is first applied and the intrinsic mode functions (IMFs) with and without mode-mixing are identified. Bandpass filtering is applied to the harvester data in the frequency bands selected by observing the Fourier spectra of the IMFs. Once the IMFs are recovered, the natural frequencies and the damping can be estimated using a combination of Natural Excitation technique and Hilbert transform respectively [35,39]. Fig. 20 show the time series, Fourier spectrum and the spectrogram of the first mode, as obtained from cantilever 4. It is observed that there is a mode in the vicinity of 9 Hz, which is corroborated by both the spectrum peak and the location of the maximum energy in the T-F plane of the scalogram.

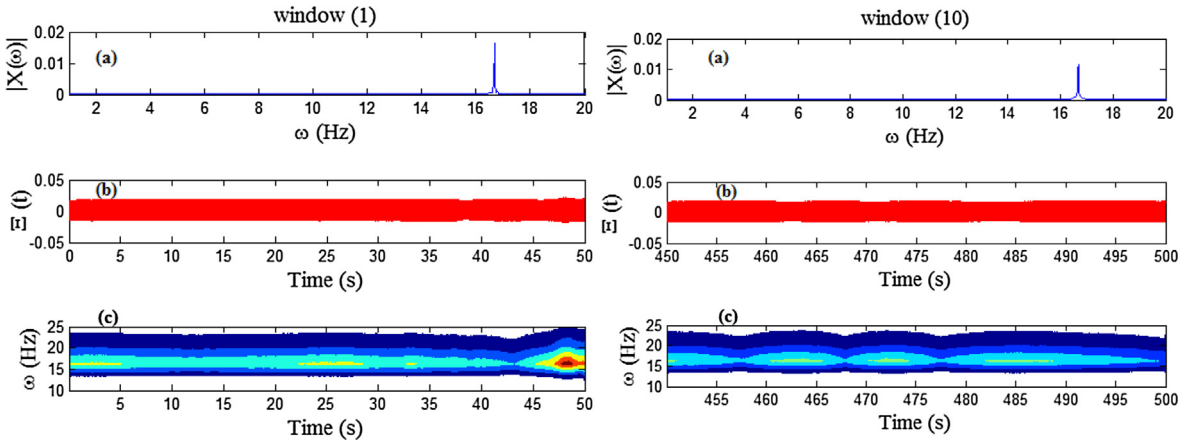

Fig. 17. (a) Spectrum, (b) Time series and (c) Scalograms of the cantilever 4 harvester data for two windows during Test 1.

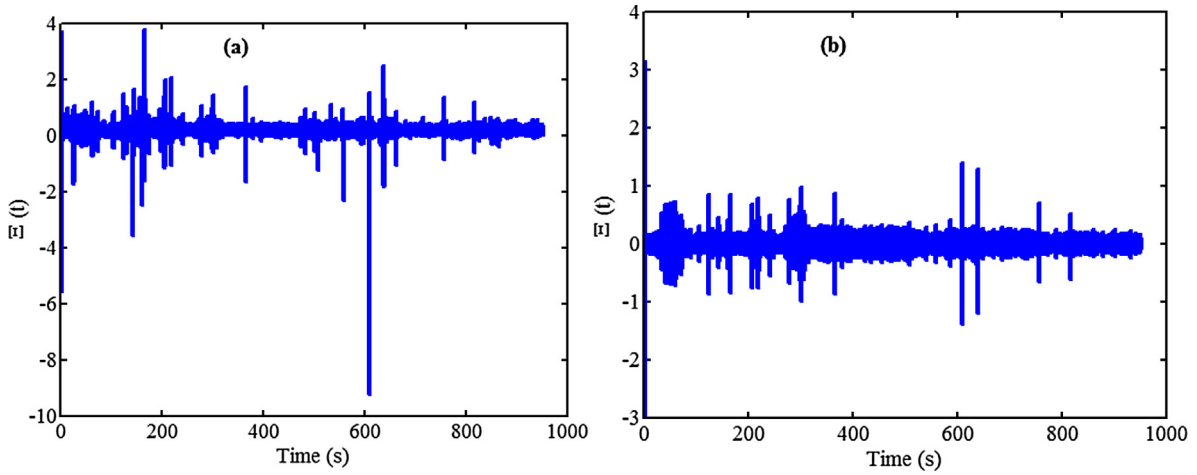

Fig. 18. Time series from Test 1 of the cantilever 4 harvester data for band-pass filtered between (a) 0–16 Hz and (b) 17–35 Hz.

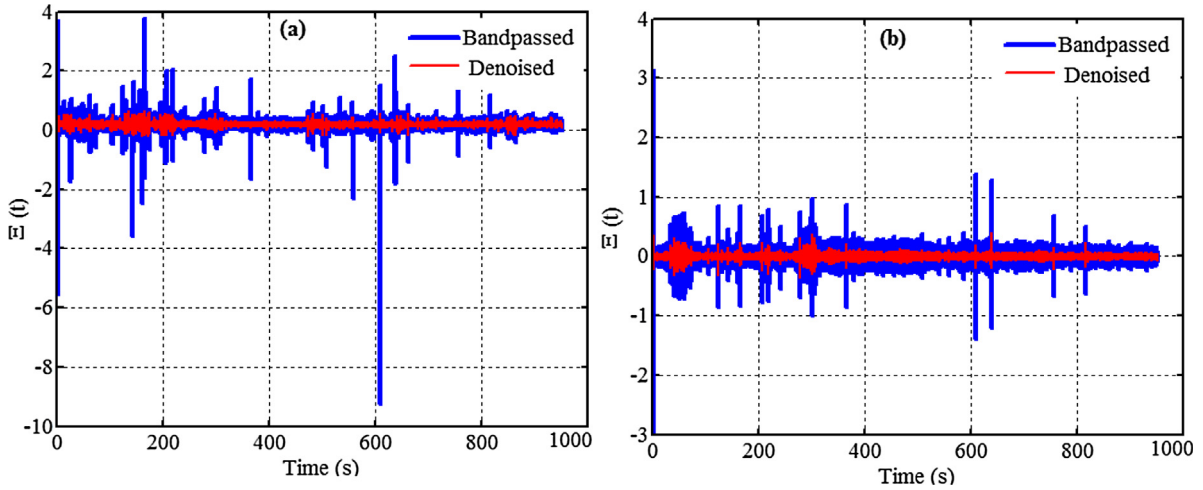

Fig. 19. Denoising of cantilever 4 harvester data, from Test 1, with band-pass filtered between (a) 0–16 Hz and (b) 17–35 Hz.

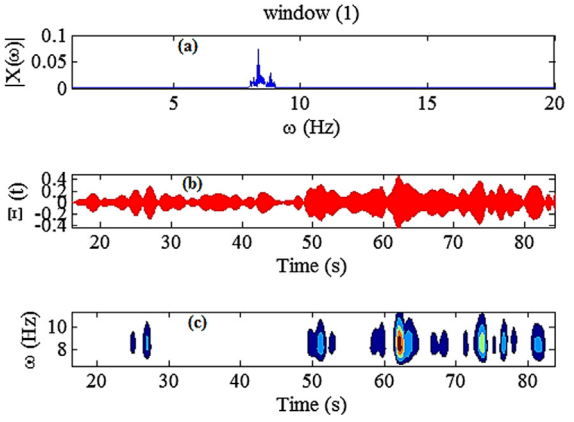

Fig. 20. (a) Fourier spectrum, (b) Time series and (c) Scalogram of Mode-1.

Table 3
Identified window-wise averaged natural frequencies from cantilever harvesters 2, 5 and 4.

Modes	Test 1			Test 3		
	Cant. 2	Cant. 5	Cant. 4	Cant. 2	Cant. 5	Cant. 4
1	8.30	8.35	8.4	8.28	8.35	8.45
2	12.20	12.40	12.45	12.25	12.44	12.53
3	15.20	15.42	15.40	15.28	15.48	15.46
4	–	19.45	19.96	–	19.35	20.00
5	–	23.0	23.28	–	23.38	23.36
6	–	–	27.12	–	–	27.00

Application of Hilbert transform on the first IMF further confirms the natural frequency as 8.4 Hz which is shown in Table 3. The time and frequency localizations of the first six modes can be observed in Fig. 21. The identified natural frequencies and the damping are shown in Table 3. The damping values are estimated using Natural Excitation technique [19]. The rationale of using the technique can be justified from the fact that although the harvester vibration encodes filtered sine sweep responses of the bridge, the presence of strong winds and gusty weather is liable to act like broad band excitation to the bridge in addition to the forced excitations.

Table 3 shows the natural frequencies identified by three harvesters using two different sweep rates. It is observed that from cantilever 4 harvester data, 6 modes can be identified followed by 5 from cantilever 5 and 3 from cantilever 2. This is expected as cantilever 2 is not able to cover as much frequency range as cantilever 4, due to their respective resonant frequencies of 8.37 Hz and 17.95 Hz respectively. The identified frequencies match up quite well with the ones identified from Pershagen bridge using acceleration data, the results of which are reported in [34]. Caution however must be exercised against over-interpretation of the identified frequencies and damping when compared against those obtained from acceleration data using sine sweep excitation as there was significant contribution from wind gusts on the quality of data obtained from the harvester, as observed in Figs. 18 and 19.

Table 4 shows the damping values identified by the three harvesters using two different sweep rates. It can be observed that most of the identified damping values lie in the 1.5–2% of critical damping ratio, which is an acceptable range for most of the large structures of the type considered in this paper. There is a slight trend of the identified damping values to be a little lesser for cantilever 2 harvester data as compared to the cantilever 4 data.

5.3. Train passage detection

Short duration events like train passages can be important in the context of short term continuous vibration monitoring of bridge structures. They are liable to cause changes that may or may not be significant in terms of the dynamic responses of the bridge due to their weight, speed and coupling with the bridge responses [40]. This is particularly important for drive-by inspections as well. Hence, detection of such events is an important step to identify the presence and the effect of such presence automatically from energy harvesting for monitoring or damage detection purposes [41]. In the present application, a framework to detect such changes is shown with the aid of condition indicators or statistical markers.

Condition indicators are statistical indicators of signal quality, which are traditionally used in fault detection, condition monitoring or change detection [19,30,36]. To detect changes in the dynamic behaviour of a system in response to sudden

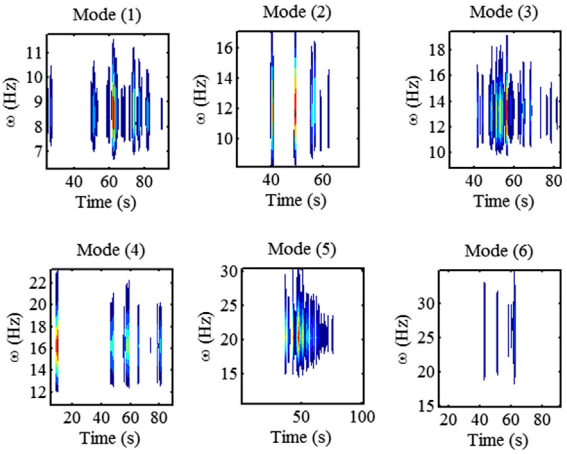

Fig. 21. Scalograms of the identified Modes.

Table 4
Identified window-wise averaged damping from cantilever harvesters 2, 5 and 4.

Modes	Test-1			Test-3		
	Cant. 2	Cant. 5	Cant. 4	Cant. 2	Cant. 5	Cant. 4
1	1.0	1.2	1.3	1.1	1.2	1.4
2	1.5	2.0	1.7	1.6	2.1	1.9
3	1.2	1.4	1.5	1.4	1.5	1.6
4	–	1.0	1.2	–	1.1	1.3
5	–	1.2	1.1	–	1.3	1.2
6	–	–	1.5	–	–	1.6

Table 5
Condition indicators used for train passage detection.

Condition indicator	Formula
Energy operator	EOP $(\chi(i)) = s(i)^2 - s(i+1)s(i-1)$
Energy operator kurtosis	$\kappa(\chi) = \frac{1}{N}\sum_{i=1}^{N} \frac{(\chi-\mu_\chi)^4}{\sigma_\chi^4}$

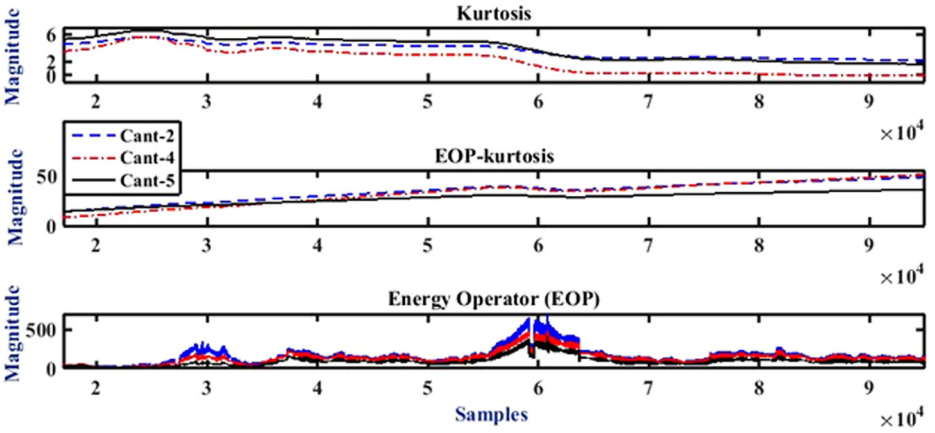

Fig. 22. Condition indicators for train passage detection.

alteration in environmental or loading conditions, recursive implementations of condition indicators is necessary [36]. This approach is motivated for situations where there are frequent changes in operating conditions that do not necessarily correspond to damage. To detect changes in harvester response data due to train passage, three established condition indicators [30,36] are chosen, namely: the energy operator, kurtosis of energy operator and kurtosis of the energy operator applied on the envelop of the harvester response. A brief description of the performance indicators is provided in Table 5. The ith sample of data series $s(i)$ with length N is considered for energy operator $\chi(i)$ and energy operator kurtosis $\kappa(\chi)$ where μ_χ and σ_χ correspond to sample mean and standard deviation respectively.

For online train passage detection, it is important that these condition indicators are estimated recursively. For details these recursive estimates, the readers are referred to existing literature [36,42]. The next step in train passage detection is the application sequential Karhunen-Loeve transform (SKLT) [36] to the estimated recursive condition indicators. The necessity of SKLT stems from the fact that it effectively fuses the information that is provided by each of the condition indicators, reinforces certain true events and suppresses outliers in a comparative framework. SKLT is a low dimensional approximation of principal component analysis, i.e., where one or at most 2 principal components are expected. The main objective is that given a set of vectors, one seeks to estimate a set of orthogonal unit vectors such that the projections of data on the subspace spanned by the vectors approximate the input vectors best in a mean square error sense. Consider a $p \times q$ data matrix $\boldsymbol{\alpha}$ for which singular value decomposition $\boldsymbol{\alpha} = \mathbf{U}\boldsymbol{\Lambda}\mathbf{V}^{\boldsymbol{T}}$ has been already computed. When a new $p \times (q + r)$ matrix $\boldsymbol{\beta}$ of r new observations becomes available, the goal is to compute the SVD of $[\boldsymbol{\alpha}\ \boldsymbol{\beta}] = \mathbf{U}^*\boldsymbol{\Lambda}^*\mathbf{V}^{*^T}$. Since SKLT is based on the computation of $\mathbf{U}^*$ and $\boldsymbol{\Lambda}^*$ only, $\mathbf{V}^*$ is not estimated. For the details of the algorithm, the readers are referred to [36].

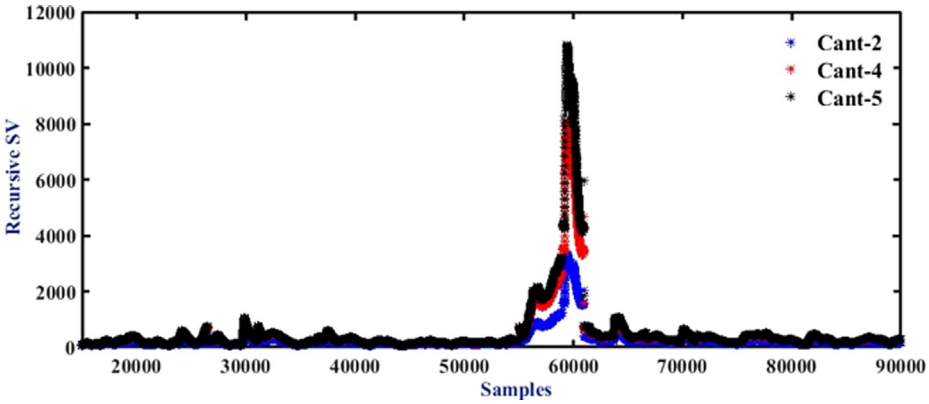

Fig. 23. Recursive singular values for train passage detection.

The aforementioned recursive condition indicators estimated from cantilever 2, 4 and 5 harvester data are shown in Fig. 22. It can be observed that the condition indicators 1 and 3 pick up some events in the vicinity of 25,000th sample whereas all the three condition indicators pick up events in the vicinity of 59,500th sample [Fig. 23], spreading over a small window. SKLT over the condition indicators further reinforces that there is indeed a strong activity in the vicinity of 59,500th sample indicating that there is an event corresponding to the small window in and around 59,500th data point. Further examination of the ground truth suggests that it is an event corresponding to the passage of a train.

6. Conclusions

This paper presents the deployment of piezoelectric energy harvesting devices in a full-scale bridge structure and subsequent monitoring while undergoing forced dynamic testing and train passages. Associated analysis techniques for system and event identification are also developed. Six energy harvesting devices were developed, with each device consisting of aluminium cantilevers and piezoelectric PVDF material. The natural frequencies of the cantilever devices were spread over a frequency range from 6.2 Hz to 20.6 Hz, to match the estimated frequency of the bridge. The development and calibration of the devices is presented in relation to the bridge tested. The deployment of the energy harvesting devices to a bridge structure is presented along with details of the host structure. To obtain the response of the bridge, forced vibration testing using a hydraulic shaker unit was carried out. Responses of the bridge was measured while it was actively excited with a swept-sinusoidal force at different amplitudes and frequency ranges, while the bridge remained operational and open to train passage. Responses of all energy harvesting cantilevers were compared for the tests along with the corresponding accelerations at the harvester location. Following this, analysis was performed on the measured responses of the energy harvesting devices. A bespoke denoising process was developed and implemented to remove external interference on the voltage output signal. A Hilbert Transform based envelop extraction led to demodulation of input data and subsequent statistical thresholding combined with a Savitzky-Golay filter based smoothing leads to a significantly denoised data, while retaining key information. Modal identification is then carried out using an empirical mode decomposition based technique and the damping estimated is obtained by averaging over several windows. The natural frequency of the bridge was determined to be between 7.79 Hz and 7.87 Hz from analysis of the measured accelerometer responses, compared against between a range of 8.3 Hz and 8.45 Hz as determined by the energy harvesters. A Sequential Karhunen Loeve Transform (SKLT) based algorithm was subsequently employed to determine events of interest in the form of train passages. The passages were successfully identified from the measured response of harvested energy.

Acknowledgements

The authors wish to acknowledge the financial support of the Irish Research Council through the Government of Ireland Postgraduate Scholarship Scheme, Grant GOIPG/2013/482, Science Foundation Ireland, through Grant 13/TIDA/I12587 and Erasmus Mundus EUPHRATES project. The authors also wish to acknowledge SFI Marine and Renewable Energy Ireland (MaREI) Centre.

References

[1] J. Brownjohn, Structural health monitoring of civil infrastructure, Phil. Trans. R. Soc. A. 365 (1851) (2007) 589–622.
[2] C. Farrar, G. Park, D. Allen, M. Todd, Sensor network paradigms for structural health monitoring, Struct. Control Hlth. 13 (1) (2006) 210–225.
[3] S. Beeby, M. Tudor, N. White, Energy harvesting vibration sources for microsystems applications', Meas. Sci. Technol. 17 (12) (2006) R175–R195.
[4] S. Anton, H. Sodano, A review of power harvesting using piezoelectric materials (2003–2006), Smart Mater. Struct. 16 (3) (2007) R1–R21.
[5] J. Matiko, N. Grabham, S. Beeby, M. Tudor, Review of the application of energy harvesting in buildings, Meas. Sci. Technol. 25 (1) (2014) 012002.

[6] S. Ali, M. Friswell, S. Adhikari, Analysis of energy harvesters for highway bridges, J. Intell. Mater. Syst. Struct. 22 (16) (2011) 1929–1938.
[7] A. Erturk, Piezoelectric energy harvesting for civil infrastructure system applications: Moving loads and surface strain fluctuations, J. Intell. Mater. Syst. Struct. 22 (17) (2011) 1959–1973.
[8] P. Cahill, N. Nuallain, N. Jackson, A. Mathewson, R. Karoumi, V. Pakrashi, Energy harvesting from train-induced response in bridges, ASCE J. Bridge Eng. 19 (9) (2014) 04014034.
[9] G. Gatti, M. Brennan, M. Tehrani, D. Thompson, Harvesting energy from the vibration of a passing train using a single-degree-of-freedom oscillator, Mech. Syst. Signal Process 66–67 (2016) 785–792.
[10] P. Cahill, R. O'Keeffe, N. Jackson, A. Mathewson, V. Pakrashi, Structural health monitoring of reinforced concrete beam using piezoelectric energy harvesting system, In: Proceedings of EWSHM-7th European Workshop on Structural Health Monitoring, 2014.
[11] P. Cahill, V. Jaksic, J. Keane, A. O'Sullivan, A. Mathewson, S. Ali, V. Pakrashi, Effect of road surface, vehicle, and device characteristics on energy harvesting from bridge–vehicle interactions, Comput.-Aided Civ. Infrastruct. Eng. 31 (12) (2016) 921–935.
[12] V. Jaksic, R. O'Shea, P. Cahill, J. Murphy, D. Mandic, V. Pakrashi, Dynamic response signatures of a scaled model platform for floating wind turbines in an ocean wave basin, Phil. Trans. R. Soc. A 373 (2035) (2015) 20140078.
[13] O. Salawu, C. Williams, Review of full-scale dynamic testing of bridge structures, Eng. Struct. 17 (2) (1995) 113–121.
[14] A. Morassi, S. Tonon, Dynamic testing for structural identification of a bridge, ASCE J. Bridge Eng. 13 (6) (2008) 573–585.
[15] J. Kim, J. Lynch, Experimental analysis of vehicle–bridge interaction using a wireless monitoring system and a two-stage system identification technique, Mech. Syst. Signal Process 28 (1) (2012) 3–19.
[16] J. Kwark, E. Choi, Y. Kim, B. Kim, S. Kim, Dynamic behavior of two-span continuous concrete bridges under moving high-speed train, Comput. Struct. 82 (4–5) (2004) 463–474.
[17] R. Karoumi, J. Wiberg, A. Liljencrantz, Monitoring traffic loads and dynamic effects using an instrumented railway bridge, Eng. Struct. 27 (12) (2005) 1813–1819.
[18] M. Ülker-Kaustell, R. Karoumi, Application of the continuous wavelet transform on the free vibrations of a steel-concrete composite railway bridge, Eng. Struct. 33 (3) (2011) 911–919.
[19] C. Farrar, G. James, System identification from ambient vibration measurements on a bridge, J. Sound Vib. 205 (1) (1997) 1–18.
[20] A. Cunha, E. Caetano, F. Magalhães, C. Moutinho, Recent perspectives in dynamic testing and monitoring of bridges', Struct. Control Hlth. 20 (6) (2013) 853–877.
[21] B. Peeters, J. Maeck, G. Roeck, Vibration-based damage detection in civil engineering: excitation sources and temperature effects, Smart Mater. Struct. 10 (3) (2001) 518–527.
[22] M. Halling, I. Muhammad, K. Womack, Dynamic field testing for condition assessment of bridge bents', ASCE J. Struct. Eng. 127 (2) (2001) 161–167.
[23] C. Farrar, D. Jauregui, Comparative study of damage identification algorithms applied to a bridge: I. Experiment, Smart Mater. Struct. 7 (5) (1998) 704–719.
[24] M. Peigney, D. Siegert, Piezoelectric energy harvesting from traffic induced bridge vibrations', Smart Mater. Struct. 22 (9) (2013) 095019.
[25] T. Galchev, J. McCullagh, R. Peterson, K. Najafi, Harvesting traffic-induced vibrations for structural health monitoring of bridges', J. Micromech. Microeng. 21 (10) (2011) 104005.
[26] E. Sazonov, D. Curry, P. Pillay, Self-powered sensors for monitoring of highway bridges', IEEE Sens. J. 9 (11) (2009) 1422–1429.
[27] K. Sekuła, P. Kołakowski, Piezo-based weigh-in-motion system for the railway transport, Struct. Control Hlth. 19 (2) (2012) 199–215.
[28] W. Fan, P. Qiao, Vibration-based damage identification methods: a review and comparative study, Struct. Health Monit. 10 (1) (2011) 83–111.
[29] V. Pakrashi, A. O'Connor, B. Basu, A study on the effects of damage models and wavelet bases for damage identification and calibration in beams, Comput.-Aided Civ. Infrastruct. Eng. 22 (8) (2007) 555–569.
[30] V. Pakrashi, B. Basu, A. O' Connor, Structural damage detection and calibration using a wavelet–kurtosis technique', Eng. Struct. 29 (9) (2007) 2097–2108.
[31] H. Xue, Y. Hu, Q. Wang, Broadband piezoelectric energy harvesting devices using multiple bimorphs with different operating frequencies, IEEE Trans. Ultrason., Ferroelect., Freq Control 55 (9) (2008) 2104–2108.
[32] N. DuToit, B. Wardle, Experimental verification of models for microfabricated piezoelectric vibration energy harvesters, AIAA J. 45 (5) (2007) 1126–1137.
[33] J. Brownjohn, P. Moyo, P. Omenzetter, Y. Lu, Assessment of highway bridge upgrading by dynamic testing and finite-element model updating, ASCE J. Bridge Eng. 8 (3) (2003) 162–172.
[34] A. Andersson, M. Ülker-Kaustell, R. Borg, O. Dymén, A. Carolin, R. Karoumi, Pilot testing of a hydraulic bridge exciter, MATEC Web Conf. 24 (2015) 02001.
[35] B. Hazra, A. Sadhu, A. Roffel, S. Narasimhan, Hybrid time-frequency blind source separation towards ambient system identification of structures, Comput.-Aided Civ. Infrastruct. Eng. 27 (5) (2012) 314–332.
[36] B. Hazra, A. Sadhu, S. Narasimhan, Fault detection of gearboxes using synchro-squeezing transform, J. Vib. Control (2016), 1077546315627242.
[37] A. Sadhu, B. Hazra, S. Narasimhan, Decentralized modal identification of structures using parallel factor decomposition and sparse blind source separation, Mech. Syst. Signal Process 41 (1–2) (2013) 396–419.
[38] Y. Yang, S. Nagarajaiah, Time-frequency blind source separation using independent component analysis for output-only modal identification of highly damped structures, ASCE J. Struct. Eng. 139 (10) (2012) 1780–1793.
[39] B. Hazra, Hybrid time and time-frequency blind source separation towards ambient system identification of structures, Ph.D. thesis, Department of Civil and Environmental Engineering, University of Waterloo, Canada, 2010, pp. 1–170.
[40] V. Pakrashi, A. O'Connor, B. Basu, Effect of tuned mass damper on the interaction of a quarter car model with a damaged bridge, Struct. Infrastruct. Eng. 6 (4) (2010) 409–421.
[41] V. Pakrashi, A. O'Connor, B. Basu, A bridge-vehicle interaction based experimental investigation of damage evolution, Struct. Health Monit. 9 (4) (2010) 285–296.
[42] M. Krishnan, B. Bhowmik, B. Hazra, V. Pakrashi, Real time damage detection using recursive principal components and time varying autoregressive modeling, Mech. Syst. Signal Process 101 (2018) 549–574.